

Strain tunable excitonic optical properties in monolayer Ga_2O_3

Hao-Lei Cui(崔浩磊), Zhen Quan(权真), and Shu-Dong Wang(王舒东)

Citation: Chin. Phys. B, 2024, 33 (**10**): 107104. DOI: 10.1088/1674-1056/ad74e7
Journal homepage: http://cpb.iphy.ac.cn; http://iopscience.iop.org/cpb

What follows is a list of articles you may be interested in

Exciton-polaritons in a 2D hybrid organic-inorganic perovskite microcavity with the presence of optical Stark effect

Kenneth Coker, Chuyuan Zheng(郑楚媛), Joseph Roger Arhin, Kwame Opuni-Boachie Obour Agyekum, and Weili Zhang(张伟利)
Chin. Phys. B, 2024, 33 (**3**): 037102. DOI: 10.1088/1674-1056/ad1484

Doublet luminescence due to coexistence of excitons and electron-hole plasmas in optically excited $CH_3NH_3PbBr_3$ single crystal

Jie Wang(王杰), Guang-Zhe Ma(马广哲), Lu Cao(曹露), Min Gao(高敏), and Dong Shi(石东)
Chin. Phys. B, 2022, 31 (**4**): 047104. DOI: 10.1088/1674-1056/ac29b5

Dynamic recombination of triplet excitons in polymer heterojunctions

Ya-Dong Wang(王亚东), Jian-Jun Liu(刘建军), Xi-Ru Wang(王溪如), Yan-Xia Liu(刘艳霞), and Yan Meng(孟艳)
Chin. Phys. B, 2020, 29 (**11**): 117101. DOI: 10.1088/1674-1056/ab9c13

Exciton dynamics in different aromatic hydrocarbon systems

Milica Rutonjski†, Petar Mali, Slobodan Rado\v sevi\'c, Sonja Gombar, Milan Panti\'c, and Milica Pavkov-Hrvojevi\'c
Chin. Phys. B, 2020, 29 (**10**): 107103. DOI: 10.1088/1674-1056/aba2de

Exciton optical absorption in asymmetric ZnO/ZnMgO double quantum wells with mixed phases

Zhi-Qiang Han(韩智强), Li-Ying Song(宋丽颖), Yu-Hai Zan(昝宇海), Shi-Liang Ban(班士良)
Chin. Phys. B, 2020, 29 (**7**): 077104. DOI: 10.1088/1674-1056/ab8d9d

---

Strain tunable excitonic optical properties in monolayer Ga_2O_3

Hao-Lei Cui(崔浩磊), Zhen Quan(权真), and Shu-Dong Wang(王舒东)†

School of Physical Science and Technology, Inner Mongolia University, Hohhot 010021, *China*

(Received 8 July 2024; revised manuscript received 24 August 2024; accepted manuscript online 29 August 2024)

Two-dimensional (2D) Ga_2O_3 has been confirmed to be a stable structure with five atomic layer thickness configuration. In this work, we study the quasi-particle electronic band structures and then access the excitonic optical properties through solving the Bethe–Salpeter equation (BSE). The results reveal that the exciton dominates the optical absorption in the visible light region with the binding energy as large as ~ 1.0 eV, which is highly stable at room temperature. Importantly, both the dominant absorption P_1 and P_2 peaks are optically bright without dark exciton between them, and thus is favorable for luminescence process. The calculated radiative lifetime of the lowest-energy exciton is 2.0×10^{-11} s at 0 K. Furthermore, the radiative lifetime under +4% tensile strain is one order of magnitude shorter than that of the strain-free case, while it is less insensitive under the compressive strain. Our findings set the stage for future theoretical and experimental investigation on monolayer Ga_2O_3.

Keywords: excitons, radiative lifetime, Ga_2O_3

PACS: 71.35.–y, 71.35.Cc, 31.15.ag, 73.43.Cd **DOI:** 10.1088/1674-1056/ad74e7

1. Introduction

Gallium oxide (Ga_2O_3) is an emerging ultra-wide bandgap ($\sim$ 4.8 eV)[1] transparent semiconducting oxide. There exist five polymorphs of Ga_2O_3, known as α, β, γ, δ, and ε.[2–7] Among these five phases of Ga_2O_3, the monoclinic β-Ga_2O_3 is the most thermodynamically stable structure and has attracted intensive research in photodetectors, optoelectronic devices, sensing systems, photocatalysts, and electrodes.[8–14] Unlike other ultra-wide bandgap semiconducting materials, such as AlGaN, AlN, and diamond which are difficult in large-scale synthesis, bulk crystal β-Ga_2O_3 can be fabricated in a large volume and low production costs.[9] These unique features promote β-Ga_2O_3 as an ideal candidate for future applications.

In addition to bulk crystal β-Ga_2O_3, low-dimensional structures, such as nanowires, nanorods, nanoribbons, nanobelts, nanosheets, and nanoparticles have been grown successfully.[9,14] Likewise, two-dimensional (2D) β-Ga_2O_3 has been obtained via mechanically exfoliated from the bulk crystal[15–18] and epitaxial growth methods.[19–21] However, the obtained 2D β-Ga_2O_3 possesses the similar physical properties to that of the bulk counterpart due to the large thickness.[15,16] Recently, a 2D five-atom-thick Ga_2O_3 has been investigated.[22–27] This 2D monolayer Ga_2O_3 adopts the same structures as experimentally synthesized 2D III–VI van der Waals (vdW) family members, e.g., Ga_2S_3 and In_2Se_3.[28–31] These III–VI structures usually have out-of-plane piezoelectricity[32] and ferroelectricity[33–35] due to the asymmetric configuration. For Ga_2O_3 monolayer, Liao *et al*. have discovered two configurations named ferroelectric wurtzite (FE-WZ′) and ferroelectric zinc blende (FE-ZB′), with the FE-ZB′a little bit stable than FE-WZ′.[23] They have also found that the electronic and optical properties can be tuned by strain, and the photoexcited electrons and holes are separated within the layer.[23] Meanwhile, a very high electron mobility in Ga_2O_3 monolayer have been reported.[23] Zhao *et al*. have revealed the transition from ferroelectric phase to antiferroelectric phase of bilayer Ga_2O_3 induced by the tensile strain.[24] Liu *et al*. have demonstrated a quite low lattice thermal conductivity of monolayer Ga_2O_3 at room temperature.[36]

In spite of having potential applications in piezoelectricity,[32] ferroelectricity,[33–35] water splitting,[37,38] gas sensing,[25,39] and optoelectronics,[40] the investigation of electron–hole interaction is still lacking. For 2D atomically thin monolayer like Ga_2O_3, the reduced dielectric screening and quantum confinement effect enhance the electron–hole Coulomb interaction, and thus electrons and holes form tightly bound excitons. The strong excitonic effect dominates the inherent optical and optoelectronic properties of 2D materials. More importantly, the exciton-related optical properties can be tuned by external stimuli, such as electric field, magnetic field, and strain, expanding the practical applications.[41–43]

In this work, we investigate the excitonic effect of monolayer Ga_2O_3 by many-body perturbation theory. We firstly computed the quasi-particle energies and then the optical absorption properties have been discussed, including the exciton radiative lifetime and the exciton binding energies. Finally, the strain tunable excitonic effect are also studied.

2. Computational and theoretical methods

The ground state properties in this work are performed using the Quantum ESPRESSO package,[44,45] based on den-

†Corresponding author. E-mail: sdwang@imu.edu.cn

© 2024 Chinese Physical Society and IOP Publishing Ltd

sity functional theory (DFT). The exchange–correlation interaction was treated by the generalized gradient approximation (GGA) of Perdew–Burke–Ernzerhof (PBE).[46] The cutoff energy for the plane-wave basis is set to 80 Ry (1 Ry = 13.6056923(12) eV). The Brillouin zone was sampled using 46×46×1 k-mesh with the Monkhorst–Pack scheme. A vacuum thickness of 25 Å was adopted along the z direction to mimic the isolated 2D system. The phonon spectra are calculated by the density functional perturbation theory (DFPT)[47] implemented in Quantum ESPRESSO package.[44,45] The optimized norm-conserving Vanderbilt pseudopotentials from PseudoDojo[48,49] are utilized for the valence electrons.

The quasi-particle energies E^{QP} are calculated within the one-shot GW approximation (G_0W_0), where G is the one-particle Green's function and W is the screened Coulomb interaction. The screening W is treated with the plasmon-pole approximation.[50] The exchange and correlation parts are cut by 60 Ry and 11 Ry, respectively, and 30 empty bands plus an extrapolar correction scheme[51] is used to converge the results. The optical absorption properties are calculated by solving the Bethe–Salpeter equation (BSE).[52,53] 5 valence and 5 conduction bands around the band edges are included for the calculation of the spectra. A 48×48×1 k-point grid of is used for the GW and BSE calculation. The excited property calculations are performed with Yambo code.[54,55]

The radiative lifetime of exciton is described by the Fermi golden rule.[56,57] At 0 K, the radiative lifetime is characterized as follows:

$$\tau_{\mathrm{S}}(0) = \gamma_{\mathrm{S}}(0)^{-1} = \frac{\hbar^2 cA}{8\pi e^2 E_{\mathrm{S}} \mu_{\mathrm{S}}^2}, \tag{1}$$

where c is the speed of light, A is the area of the unit cell, E_{S} is the excitation energy, and μ_{S} is the transition dipole moment of the exciton obtained from the BSE results. For finite temperature, the lifetime is given by

$$\langle \tau_{\mathrm{S}} \rangle (T) = \gamma_{\mathrm{S}}(0)^{-1} \times \frac{3}{4} \left(\frac{2M_{\mathrm{S}} c^2 k_{\mathrm{B}} T}{E_{\mathrm{S}}^2} \right), \tag{2}$$

where k_{B} is the Boltzmann constant, T is temperature, and M_{S} is the effective mass of the exciton deduced from the quasi-particle energies.

3. Results and discussion

In Fig. 1 we show the optimized structure of monolayer Ga_2O_3 and the phonon dispersion spectrum. The relaxed lattice parameter is $a = b = 3.08$ Å in the primitive hexagonal unit cell by GGA-PBE, agreeing well with the previous results.[23,36] The breaking of centrosymmetry of monolayer Ga_2O_3 introduces an intrinsic electric field [indicated by the arrow in Fig. 1(a)], analogous to the Janus TMDs,[58] which facilitates the photocatalysis.[37,59] The calculated dipole moment is 0.547 Debye (1 Debye = 3.33564×10^{-30} C·m), with the direction is opposite to that of the electric field shown in Fig. 1(a). The phonon dispersion spectrum in Fig. 1(b) demonstrates the dynamical stability of monolayer Ga_2O_3. Also, previous results reveal that the dynamic stability of monolayer Ga_2O_3 can be maintained even applying a large tensile strain of +6%.[23]

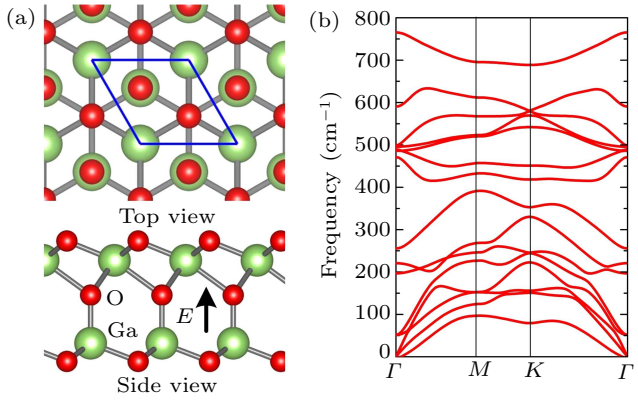


Fig. 1. Top and side views of monolayer Ga_2O_3 (a) and the phonon dispersion (b). The primitive cell is labeled by the blue solid line. The black arrow denotes the intrinsic electric field. The Ga/O atom is depicted by green (big)/red (small).

Figure 2 presents the projected and quasi-particle band structures of monolayer Ga_2O_3. The monolayer Ga_2O_3 is a indirect band gap semiconductor, with the conduction band minimum (CBM) locating at the Γ point, mainly contributed by the s orbitals of O and Ga atoms, as shown in Fig. 2(a). The p_z orbitals of O atoms dominate the valence band minimum (VBM) at the K point [Fig. 2(d)]. The p_x and p_y orbitals of O atoms and some of the d orbitals of Ga atom contribute to the VBs at the Γ point. The calculated direct band gap is 1.94 eV at the Γ point, and indirect gap is 1.45 eV between the K and the Γ points by DFT-PBE. A striking feature is the significant difference in effective mass between electrons and holes, which is reflected by the dispersive conduction bands and the relative flat valence bands around the gap. The quasi-particle band structure is presented in Fig. 2(o) for the strain-free Ga_2O_3, where the indirect band gap characteristic turns into direct band gap one, with the GW gap of 3.52 eV. Under the compressive of −4%, there also exist an indirect band to direct band gap transition compared to the PBE results, shown in Fig. 2(n), in which the valence bands around the Γ point move upward with respective to the pristine structure. The reason for this is that the valence bands around the Γ point are dominated by the in-plane p_x and p_y orbitals of O atoms, and the biaxial compressive strain modifies these in-plane orbitals. Furthermore, a compressive strain of −4% can overcome the energy difference of 0.1 eV between the K and the Γ points of the highest valence band, resulting in an indirect band to direct band gap (3.64 eV) transition. When applying the tensile strain of 4%, the band structure keeps its indirect bang gap (2.77 eV) feature, as shown in Fig. 2(p), while the direct band gap at the Γ point decreases to 3.17 eV.

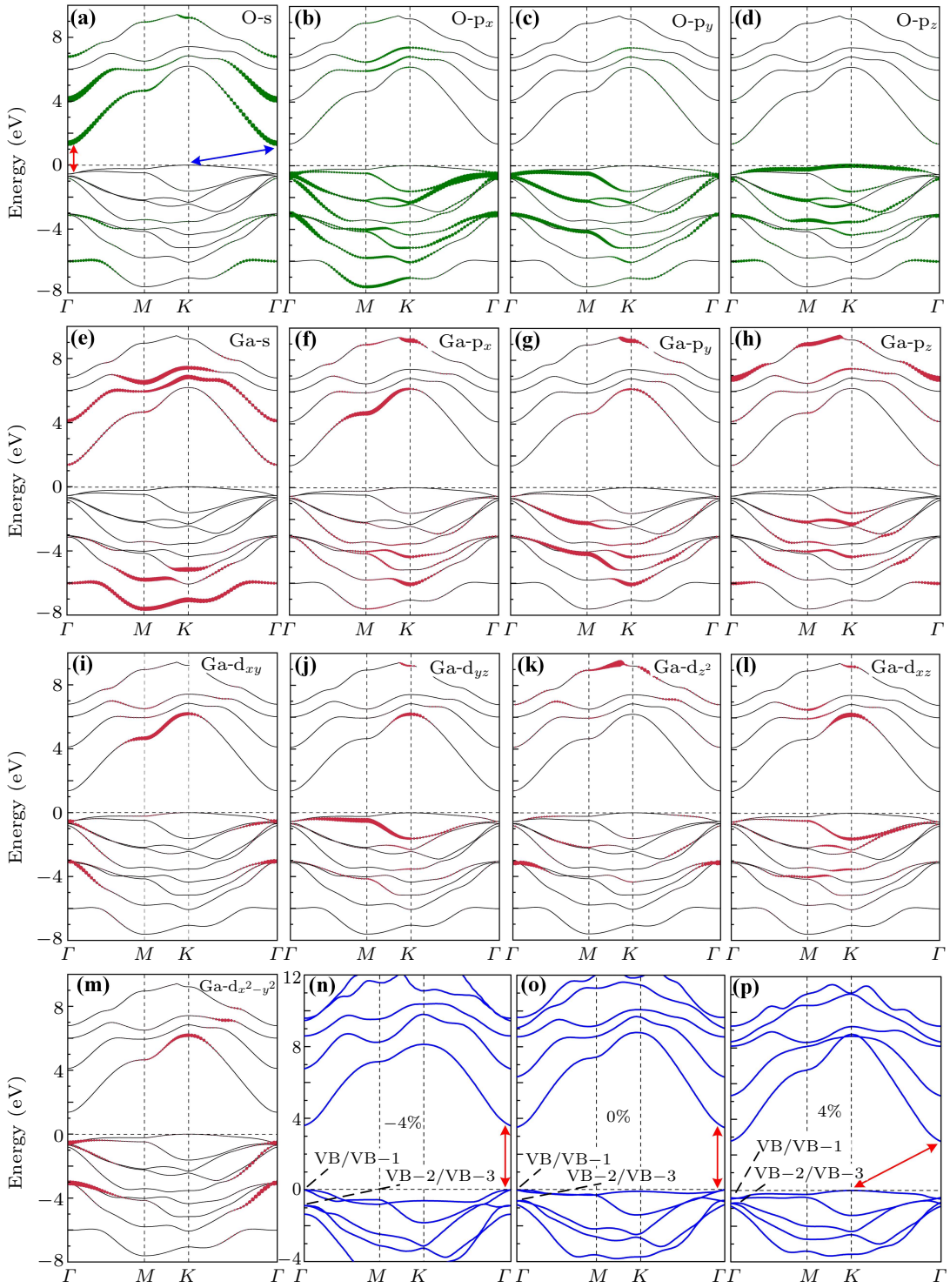


Fig. 2. Projected DFT-PBE [(a)–(m)] and quasi-particle band structures with/without biaxial strain [(n)–(p)] of monolayer Ga_2O_3. The red and blue arrows present the direct and indirect band gap, respectively. The VB, VB-1, VB-2, and VB-3 are marked out.

In Fig. 3 we present the optical absorption spectra with the inclusion of electron–hole interaction by solving the BSE. Both dominant P_1 and P_2 peaks, with/without strains, are composed of two degenerate bound excitons due to the degenerate valence bands at the Γ point, as shown in Fig. 2. For strain-free Ga_2O_3, the first (the lowest-energy) absorption peak P_1 located at 2.57 eV is contributed from the transitions of VB to CB and VB-1 to CB, while for the peak P_2, the VB-2 also participates in the transitions, giving rise to an excitation energy separation of 0.16 eV between P_1 and P_2 peaks. The exciton binding energy composed of peak P_1 is 0.96 eV, with the exciton radiative lifetime 2.3×10^{-8} s at 77 K (2.0×10^{-11} s at 0 K). Under -4% compressive strain, the peak P_1 locates at 2.58 eV, with the exciton binding energy of 1.06 eV. This peak position has a slight blue-shift compared to the strain-free structure, owing to the minor changes of the band gap between CB and VB/VB-1 at the Γ point under compressive strain. On the contrary, the peak P_2 experiences a significant moving toward

high-energy regions, as large as 0.18 eV compared to that of the structure without strain. As shown in Fig. 2(n), the large splitting between VB/VB-1 and VB-2/VB-3 under compressive strain causes the more obvious separation between P_1 and P_2. The radiative lifetime related to the lowest-energy exciton is 6.3×10^{-8} s at 77 K (3.9×10^{-11} s at 0 K), slightly longer than that of strain-free structure. After applying tensile strain of +4%, P_1 and P_2 peaks get more closer (0.11 eV), and both of them undergo a red shift compared to the pristine structure due to the reduced band gap, as shown in Fig. 3(b). Most strikingly, the oscillator strength under tensile strain is remarkably enhanced, and the intensity of P_1 is higher than in P_2. The tensile strain renders the valence bands more closely together at the Γ point, and thus the more degenerate valence bands participate in the transitions related to P_1 and P_2 peaks.

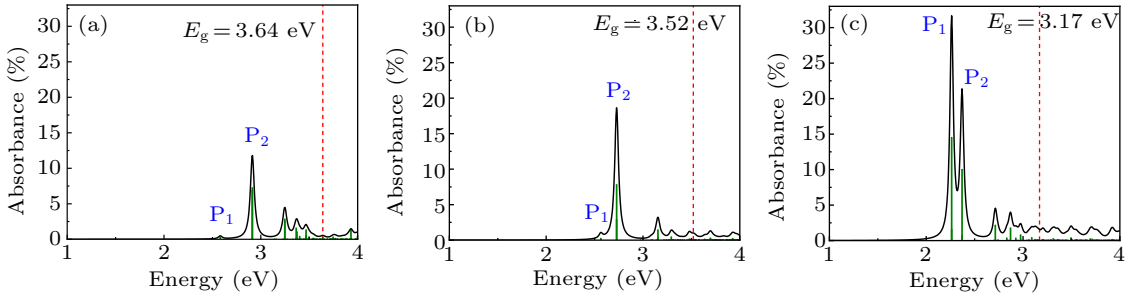


Fig. 3. Optical absorption spectra with compressive strain of −4% (a), without strain (b), and tensile strain of 4% (c). The vertical red dashed lines illustrate the quasi-particle band gap, and the P_1 and P_2 are the first two absorption peaks with the lowest energy, respectively.

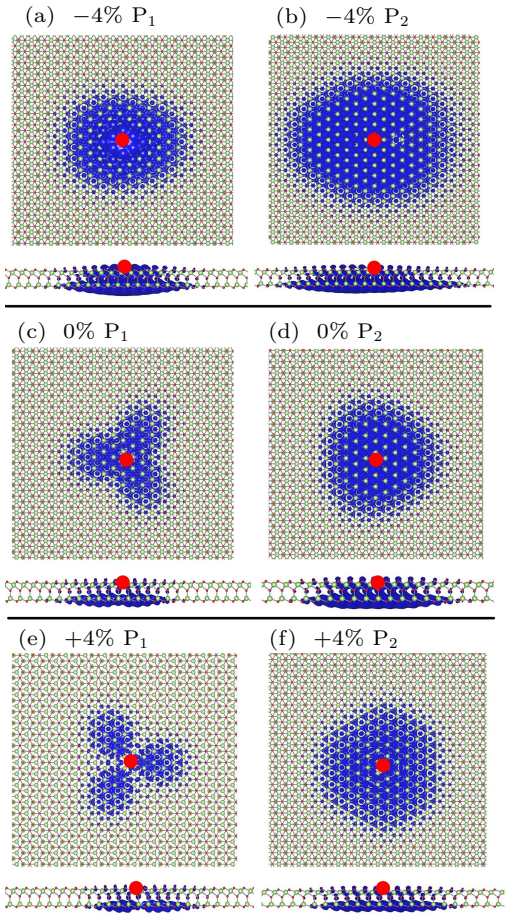


Fig. 4. Top and side views of the wave functions for excitons P_1 and P_2 in real space with/without strain. The hole position is indicated by the red circle and the blue areas indicate the distributed electrons.

The height of peak, e.g., the oscillator strengths relate to the joint density of states, JDOS. For monolayer Ga_2O_3, the tensile strain significantly alters valence bands states at the Γ point (as shown in Figs. 2(n)–2(p), the valence bands at the Γ point become more flat from −4% to 4% strains), and thus the more degenerate valence bands participate in the transitions related to P_1 and P_2 peaks, making the peaks more higher. The binding energy of the exciton in P_1 is 0.91 eV, with the radiative lifetime of 1.7×10^{-9} s at 77 K (1.3×10^{-12} s at 0 K), one order shorter than that of the strain-free case due to the large oscillator strength. In general, our calculated results discover that all the dominant peaks P_1 and P_2 reside in the visible light region, and the excitons that contribute to the dominant peaks are optically bright, and further there is no optically dark exciton between P_1 and P_2. These characteristics are beneficial for luminescence.

We now discuss the real space excitonic wave functions for P_1 and P_2, as shown in Fig. 4. Considering the excitonic wave function distributions, we can find that the electron has a high probability to be found on the lower part of monolayer Ga_2O_3, while the hole is localized in the O atom of the upper part. For exciton P_1, the wave function overlap between the electron and hole is much stronger under −4% compressive strain than that other two cases, leading to a more larger binding energy. We also notice that the excitonic wave functions for P_1 and P_2 have different symmetry features, and compressive strain of −4% significantly alters the exciton distributions while tensile strain of +4% almost maintains them. These results indicate that strain can not only tune the electronic structure, but also alter the spatial distribution state of excitons in monolayer Ga_2O_3.

4. Conclusion

In this work, we investigated electronic and optical properties of monolayer Ga_2O_3 using state-of-the-art first principles calculations. We discover that the exciton dominates the optical absorption in the visible light region with the binding

energy as large as ~ 1.0 eV, which is very stable at room temperature. Importantly, both the dominant absorption P_1 and P_2 peaks are optically bright without dark exciton between them, and thus is favorable for luminescence process. The calculated radiative lifetime of the lowest-energy exciton is 2.33×10^{-8} s at 77 K (2.0×10^{-11} s at 0 K). In the case of applied strain, we find the $+4\%$ tensile strain can significantly alter the optical absorption spectra, resulting in a large enhancement of the oscillator strength than pristine and compressive strain. Furthermore, the radiative lifetime under $+4\%$ tensile train is one order of magnitude shorter than that of the strain-free case, while it is less insensitive under the compressive strain of -4%. Our findings build the platform for future theoretical and experimental investigation on monolayer Ga_2O_3.

Acknowledgement

Project supported by the National Natural Science Foundation of China (Grant No. 12064032).

References

[1] Orita M, Ohta H, Hirano M and Hosono H 2000 *Appl. Phys. Lett.* **77** 4166
[2] Kohn J, Katz G and Broder J D 1956 *Am. Mineral.* **42** 398
[3] Saurat M and Revcolevschi A 1971 *Rev. Int. Hautes. Refract.* **8** 291
[4] He H, Blanco M A and Pandey R 2006 *Appl. Phys. Lett.* **88** 261904
[5] He H, Orlando R, Blanco M A, Pandey R, Amzallag E, Baraille I and Rerat M 2006 *Phys. Rev. B* **74** 195123
[6] Peelaers H and Van de Walle C G 2017 *Phys. Rev. B* **96** 081409
[7] Liu Y, Wang P, Yang T, Wu Q, Yang Y T and Zhang Z Y 2022 *Chin. Phys. B* **31** 117305
[8] Xi Z Y, Yang L L, Shu L C, Zhang M L, Li S, Shi L, Liu Z, Guo Y F and Tang W H 2023 *Chin. Phys. B* **32** 088502
[9] Galazka Z 2018 *Semicond. Sci. Technol.* **33** 113001
[10] Von Wenckstern H 2017 *Adv. Electron. Mater.* **3** 1600350
[11] Kim M, Seo J H, Singisetti U and Ma Z 2017 *J. Mater. Chem. C* **5** 8338
[12] Li Y, Tokizono T, Liao M, Zhong M, Koide Y, Yamada I and Delaunay J J 2010 *Adv. Funct. Mater.* **20** 3972
[13] Jin S, Wang X, Wang X, Ju M, Shen S, Liang W, Zhao Y, Feng Z, Playford H Y, Walton R I and Li C 2015 *J. Phys. Chem. C* **119** 18221
[14] Pearton S J, Yang J, Cary P H, Ren F, Kim J, Tadjer M J and Mastro M A 2018 *Appl. Phys. Rev.* **5** 011301
[15] Zhou H, Maize K, Qiu G, Shakouri A and Ye P D 2017 *Appl. Phys. Lett.* **111** 092102
[16] Kwon Y, Lee G, Oh S, Kim J H, Pearton S J and Ren F 2017 *Appl. Phys. Lett.* **110** 131901
[17] Dong L, Zhou S, Gong L, Wang W, Zhang L, Yang C, Yu J and Liu W 2020 *J. Mater. Chem. C* **8** 12551
[18] Barman S K and Huda M N 2019 *Phys. Status Solidi RRL* **13** 1800554
[19] Zavabeti A, Ou J Z, Carey B J, Syed N, Orrell-Trigg R, Mayes E L H, Xu C, Kavehei O, O'Mullane A P, Kaner R B, Kalantar-zadeh K and Daeneke T 2017 *Science* **358** 332
[20] Chandiran A K, Tetreault N, Humphry-Baker R, Kessler F, Baranoff E, Yi C, Nazeeruddin M K and Grätzel M 2012 *Nano Lett.* **12** 3941
[21] Zhang T, Li Y, Zhang Y, Feng Q, Ning J, Zhang C, Zhang J and Hao Y 2021 *J. Alloys Compd.* **859** 157810
[22] Zhao J, Byggmästar J, Zhang Z, Djurabekova F, Nordlund K and Hua M 2021 *Phys. Rev. B* **104** 054107
[23] Liao Y, Zhang Z, Gao Z, Qian Q and Hua M 2020 *ACS Appl. Mater. Interfaces* **12** 30659
[24] Zhao J, Wang X, Chen H, Zhang Z and Hua M 2022 *Chem. Mater.* **34** 3648
[25] Zhao J, Huang X, Yin Y, Liao Y, Mo H, Qian Q, Guo Y, Chen X, Zhang Z and Hua M 2021 *J. Phys. Chem. Lett.* **12** 5813
[26] Deng Z 2022 *Phys. Chem. Chem. Phys.* **24** 13671
[27] Jin C, Tang X, Sun Q, Mu C, Krasheninnikov A V and Kou L 2024 *J. Phys. Chem. Lett.* **15** 2650
[28] Zheng Y, Tang X, Wang W, Jin L and Li G 2021 *Adv. Funct. Mater.* **31** 2008307
[29] Liu H F, Antwi K K A, Yakovlev N L, Tan H R, Ong L T, Chua S J and Chi D Z 2014 *ACS Appl. Mater. Interfaces* **6** 3501
[30] Zhou J, Zeng Q, Lv D, Sun L, Niu L, Fu W, Liu F, Shen Z, Jin C and Liu Z 2015 *Nano Lett.* **15** 6400
[31] Almeida G, Dogan S, Bertoni G, Giannini C, Gaspari R, Perissinotto S, Krahne R, Ghosh S and Manna L 2017 *J. Am. Chem. Soc.* **139** 3005
[32] Xue F, Zhang J, Hu W, Hsu W T, Han A, Leung S F, Huang J K, Wan Y, Liu S, Zhang J, He J H, Chang W H, Wang Z L, Zhang X and Li L J 2018 *ACS Nano* **12** 4976
[33] Cui C, Hu W J, Yan X, Addiego C, Gao W, Wang Y, Wang Z, Li L, Cheng Y, Li P, Zhang X, Alshareef H N, Wu T, Zhu W, Pan X and Li L J 2018 *Nano Lett.* **18** 1253
[34] Ding W, Zhu J, Wang Z, Gao Y, Xiao D, Gu Y, Zhang Z and Zhu W 2017 *Nat. Commun.* **8** 14956
[35] Xiao J, Zhu H, Wang Y, Feng W, Hu Y, Dasgupta A, Han Y, Wang Y, Muller D A, Martin L W, Hu P and Zhang X 2018 *Phys. Rev. Lett.* **120** 227601
[36] Liu G, Zhang Z, Wang H, Li G, Wang J and Gao Z 2021 *J. Appl. Phys.* **130** 105106
[37] Fu C F, Sun J, Luo Q, Li X, Hu W and Yang J 2018 *Nano Lett.* **18** 6312
[38] Zhao P, Ma Y, Lv X, Li M, Huang B and Dai Y 2018 *Nano Energy* **51** 533
[39] Xie Z, Yang F, Xu X, Lin R and Chen L 2018 *Front. Chem.* **6** 430
[40] Jacobs-Gedrim R B, Shanmugam M, Jain N, Durcan C A, Murphy M T, Murray T M, Matyi R J, Moore II R L and Yu B 2014 *ACS Nano* **8** 514
[41] Xiao J, Zhao M, Wang Y and Zhang X 2017 *Nanophotonics* **6** 1309
[42] Mueller T and Malic E 2018 *npj 2D Materilas and Applications* **2** 29
[43] Regan E C, Wang D, Paik E Y, Zeng Y, Zhang L, Zhu J, MacDonald A H, Deng H and Wang F 2022 *Nature Reviews Materials* **7** 778
[44] Giannozzi P, Baroni S, Bonini N, Calandra M, Car R, Cavazzoni C, Ceresoli D, Chiarotti G L, Cococcioni M, Dabo I, *et al.* 2009 *J. Phys.: Condens. Matter* **21** 395502
[45] Giannozzi P, Andreussi O, Brumme T, Bunau O, Buongiorno Nardelli M, Calandra M, Car R, Cavazzoni C, Ceresoli D, Cococcioni M, *et al.* 2017 *J. Phys.: Condens. Matter* **29** 465901
[46] Perdew J P, Burke K and Ernzerhof M 1996 *Phys. Rev. Lett.* **77** 3865
[47] Sohier T, Calandra M and Mauri F 2017 *Phys. Rev. B* **96** 075448
[48] Hamann D R 2013 *Phys. Rev. B* **88** 85117
[49] van Setten M J, Giantomassi M, Bousquet E, Verstraete M J, Hamann D R, Gonze X and Rignanese G M 2018 *Comput. Phys. Commun.* **226** 39
[50] Godby R W and Needs R J 1989 *Phys. Rev. Lett.* **62** 1169
[51] Bruneval F and Gonze X 2008 *Phys. Rev. B* **78** 085125
[52] Albrecht S, Reining L, Del Sole R and Onida G 1998 *Phys. Rev. Lett.* **80** 4510
[53] Rohlfing M and Louie S G 2000 *Phys. Rev. B* **62** 4927
[54] Marini A, Hogan C, Grüning M and Varsano D 2009 *Comput. Phys. Commun.* **180** 1392
[55] Sangalli D, Ferretti A, Miranda H, Attaccalite C, Marri I, Cannuccia E, Melo P, Marsili M, Paleari F, Marrazzo A, *et al.* 2019 *J. Phys.: Condens. Matter* **31** 325902
[56] Palummo M, Bernardi M and Grossman J C 2015 *Nano Lett.* **15** 2794
[57] Chen H Y, Jhalani V A, Palummo M and Bernardi M 2019 *Phys. Rev. B* **100** 075135
[58] Lu A Y, Zhu H, Xiao J, Chuu C P, Han Y, Chiu M H, Cheng C C, Yang C W, Wei K H, Yang Y, Wang Y, Sokaras D, Nordlund D, Yang P, Muller D A, Chou M Y, Zhang X and Li L J 2017 *Nat. Nanotechnol.* **12** 744
[59] Xia C, Xiong W, Du J, Wang T, Peng Y and Li J 2018 *Phys. Rev. B* **98** 165424